AEM
Journals.ASM.org

Effects of Relative Humidity and Spraying Medium on UV Decontamination of Filters Loaded with Viral Aerosols

Myung-Heui Woo,[a] Adam Grippin,[b] Diandra Anwar,[b] Tamara Smith,[a] Chang-Yu Wu,[a] and Joseph D. Wander[c]

Department of Environmental Engineering Sciences, University of Florida, Gainesville, Florida, USA[a]; Department of Chemical Engineering, University of Florida, Gainesville, Florida, USA[b]; and Air Force Research Laboratory, Tyndall Air Force Base, Florida, USA[c]

Although respirators and filters are designed to prevent the spread of pathogenic aerosols, a stockpile shortage is anticipated during the next flu pandemic. Contact transfer and reaerosolization of collected microbes from used respirators are also a concern. An option to address these potential problems is UV irradiation, which inactivates microbes by dimerizing thymine/uracil in nucleic acids. The objective of this study was to determine the effects of transmission mode and environmental conditions on decontamination efficiency by UV. In this study, filters were contaminated by different transmission pathways (droplet and aerosol) using three spraying media (deionized water [DI], beef extract [BE], and artificial saliva [AS]) under different humidity levels (30% [low relative humidity {LRH}], 60% [MRH], and 90% [HRH]). UV irradiation at constant intensity was applied for two time intervals at each relative humidity condition. The highest inactivation efficiency (IE), around 5.8 logs, was seen for DI aerosols containing MS2 on filters at LRH after applying a UV intensity of 1.0 mW/cm^2 for 30 min. The IE of droplets containing MS2 was lower than that of aerosols containing MS2. Absorption of UV by high water content and shielding of viruses near the center of the aggregate are considered responsible for this trend. Across the different media, IEs in AS and in BE were much lower than in DI for both aerosol and droplet transmission, indicating that solids present in AS and BE exhibited a protective effect. For particles sprayed in a protective medium, RH is not a significant parameter.

The increasing threat of bioterrorist attacks (e.g., *Bacillus anthracis*) and recent outbreaks of airborne pathogenic infections (e.g., severe acute respiratory syndrome) have raised the level of public interest in biological aerosols and protection methods that prevent their spread (7, 20, and http://www.cdc.gov/h1n1flu/update.htm). Filtering facepiece respirators (FFRs) certified by the National Institute for Occupational Safety and Health (NIOSH) are mandated by OSHA under 42 CFR 84 to be worn by health care personnel and are recommended as a protective device for the general public during a pandemic event. Several factors influence the effectiveness of the intended protection offered by the FFRs, including the bioaerosol transmission mode and environmental conditions (4).

Because aerosol size is a pivotal parameter for filtration efficiency, understanding the transmission mode of viral aerosols is critical to protection of the public against infection by major airborne pathogens. Three critical transmission modes are recognized for the spread of infectious viruses (4). The first is droplet transmission, which results from infected individuals generating droplets containing microorganisms by coughing, sneezing, singing, and talking. Droplets of various sizes produced by an infected person are propelled short distances through the air to a susceptible host, and the infection occurs through droplet contact with a mucous membrane. The second mode is aerosol transmission, which includes the dispersion of droplet nuclei that remain airborne after evaporation of droplets. Owing to the small size of the inhalable droplet nuclei, disease can be widely spread by this mode. The third mode is fomite transmission, which includes indirect contact through a contaminated object (e.g., towel or mask). Controlling this mode is a chronic problem in health care facilities.

As implied above, the FFR is a device that efficiently captures viruses transmitted by droplet and droplet nuclei modes. However, infectivity of the captured viruses persists, which makes the contaminated FFR a fomite. In addition, reaerosolization of viruses captured on the FFR is a possibility; transient, high rates of airflow (e.g., coughing and sneezing) aggravate the probability of reaerosolization (21). NIOSH projected that during a 42-day influenza pandemic the health care sector alone would require over 90 million masks, a demand that could create a supply shortage that would leave millions in unnecessary danger of infection (4). One possible buffer against this threat, recovering and reusing FFRs after inactivating the viruses that they capture and thus allowing them to be reused several times, has been shown to be technically feasible (10) and appears consistent with 29 CFR 1910.134(h)(1)(21). However, there is imprecision in the definition of the term "single-use" as applied to disposable N95 FFRs; for instance, the Centers for Disease Control and Prevention (CDC) recommend continuous or intermittent wearing for no more than 8 h and only until the mask becomes wet, dirty, or contaminated, ceases to seal to the wearer's face, or develops elevated flow resistance (http://www.cdc.gov/niosh/topics/respirators). The specification in 29 CFR 1910.134(d)(1)(ii), that respirators must be NIOSH certified (http://www.osha.gov/pls/oshaweb/owadisp.showdocument?pid=12716&p_table=standards), a certification that applies only to new disposable respirators, poses a procedural obstacle to implementation of this concept—even in a declared emergency (http://www.fda.gov/RegulatoryInformation/Guidances/ucm125127.htm)—that remains to be resolved.

Decontamination of used FFRs plays an important part in preventing both reaerosolization of viral particles collected on a filter

Received 16 February 2012 **Accepted** 30 May 2012
Published ahead of print 8 June 2012
Address correspondence to Chang-Yu Wu, cywu@ufl.edu.

doi:10.1128/AEM.00465-12

surface and fomite transmission, and it may extend the service lifetime of the FFRs (4). Several inactivation methods, including microwave irradiation, UV irradiation, and biocidal surfaces (9, 15, 25, 29, 34), have been shown to decontaminate viral aerosols collected on filters. These methods do not remove accumulated particles; however, loading is typically light enough that the decontaminated filter's performance is not affected. Antimicrobial agents such as phenols, alcohols, heavy metals, and quaternary ammonium compounds can be incorporated into air filters; however, the biocidal filters that have been tested release small quantities of toxic chemicals (15, 23, 33), as can chloramines (F. J. Madeline, personal communication). The use of direct microwave irradiation to kill microorganisms through thermal and nonthermal effects has also been demonstrated in various studies of solid media, but this method requires a microwave absorber (typically water, activated carbon, or silicon carbide) and may damage the material (9, 10, 21, 34).

UV-C irradiation is a recognized method that delivers sufficient energy to be a practical antimicrobial method for inactivating a wide variety of biological agents (5, 10, 17, 31). Many studies have reported that UV intensity, exposure time, lamp placement, and air movement patterns influence its inactivation efficiency (IE) against microbes (5, 13, 23, 28). However, none has considered other important parameters (e.g., relative humidity [RH], nebulized medium, and transmission mode) that influence susceptibility of viral agents collected on fibrous filters.

The objective of this study was to investigate the IE of UV irradiation against viruses collected through different transmission modes under various environmental conditions. For this, the filters were contaminated by two pathways (droplet and aerosol) using three spraying media (i.e., deionized [DI] water, beef extract in filtered, sterile DI water [BE], and an artificial saliva [AS]) at three RH conditions (i.e., low [LRH; 30% ± 5%], medium [MRH; 60% ± 5%], and high [HRH; 90% ± 5%]). UV irradiation was applied at a constant intensity of 1.0 mW/cm^2 for different time intervals.

MATERIALS AND METHODS

Preparation of MS2 and plaque assay. MS2 bacteriophage (MS2; ATCC 15597-B1) was used as the test agent. MS2 (diameter Φ, 27.5 nm) has a nonenveloped, icosahedral capsid and is commonly used as a nonpathogenic surrogate for human-pathogenic viruses (e.g., poliovirus, rotavirus, and rhinovirus) for the following reasons: physical characteristics similar to those of human-pathogenic viruses, need of only biosafety level 1 (BSL-1) containment, and ease of preparation and assay (2, 21). Nonenveloped MS2 phage was used for the worst-case scenario, because nonenveloped viruses are more resistant to a variety of inactivation treatments, including UV exposure, than enveloped viruses (2, 20). A freeze-dried MS2 culture was suspended in DI water at a titer of approximately 10^{11} to 10^{12} PFU/ml, and this stock was stored at 4°C. The virus stock was successively diluted to 10^8 to 10^9 PFU/ml with 1× phosphate-buffered saline (PBS) and used for the experiment.

A single-layer bioassay with a host of *Escherichia coli* (ATCC 15597) was used to enumerate the infectious viruses (8). Tryptone soy broth (TSB) and culture medium 271 were prepared by following the American Type Culture Collection (ATCC) procedure for MS2 assay. Freeze-dried *E. coli* cells were suspended in 1× phosphate-buffered saline (PBS), inoculated into a solidified agar plate (1.5% agar) with a sterilized loop, and incubated at 37°C overnight. The single colony from the plate was transferred into TSB and set to grow at 37°C overnight. Culture medium 271 (100 ml) was inoculated with 0.3 ml of the *E. coli* culture from TSB and incubated at 37°C for 3 h. A 1-ml aliquot of inoculated *E. coli* culture was added to a sterile conical tube containing 9 ml of soft agar (0.5% agar) in a water bath between 40 and 50°C. One milliliter of MS2 was added to the tube containing *E. coli* and agar, the mixture was shaken thoroughly, and then it was poured into a petri dish. To attain the countable range of 30 to 300 PFU/ml, serially diluted MS2 samples were used.

Spraying media. Three types of spraying media were tested: DI water, BE, and AS. DI water was included to explore properties of the naked virus. BE (0.3%) was used to simulate foreign particles, which can also contribute to encasement. Beef extract is a mixture of peptides, amino acids, nucleotide fractions, organic acids, minerals, and some vitamins, and it is derived from infusion of beef (6). Saliva is a very dilute fluid, composed of more than 98% water, electrolytes, mucus, and enzyme. AS (0.3% mucin from porcine stomach [M1778; Sigma-Aldrich] as a mucus simulant plus around 0.3% salts as electrolytes in DI water) was used to mimic human respiratory fluid and saliva (32). Mucin, a viscous glycoprotein comprising approximately 75% carbohydrate and 25% amino acids linked via glycosidic bonds between *N*-acetylgalactosamine and serine or threonine residues, readily forms a gel in water (26). A variety of inorganic ions, such as sodium, chloride, potassium, calcium, magnesium, bicarbonate, and phosphate, maintain osmotic balance and offer buffering (32).

Droplet and aerosol loading system. The experimental setup for loading droplets and aerosols containing viruses onto the substrate is displayed in Fig. 1A and B, respectively. A 2.4-MHz ultrasonic nebulizer (241T; Sonear, Farmingdale, NY) was used to generate droplets containing viruses with a flow rate of 2 liters/min. The MS2 suspension in the reservoir was prepared by dispersing 1 ml of stock solution in 25 ml of spraying medium (i.e., DI water, BE, or AS). The relatively higher titer compared to real-life conditions was used to provide concentrations above the detection limit and to shorten the experimental time. Circular coupons (diameter Φ, 2.54 cm) were cut from a 3M 1870 (NIOSH-certified N95) FFR. The droplets produced entered the chamber and were loaded onto the surface of FFR coupons for 5 min. Each filter was then cut into four equal quadrants for UV exposure. Droplet size is affected by environmental conditions such as RH and temperature. Loading of droplets onto filter coupons was conducted at room temperature (20 ± 3°C) and HRH.

A Collison nebulizer (CN25; BGI Inc., Waltham, MA) was used to generate the aerosol containing viruses with a flow rate of 6 liters/min. The MS2 suspension in the nebulizer was prepared by dispersing 2 ml of viral stock suspension in 50 ml of nebulizer medium. The aerosol from the nebulizer entered the mixing chamber and was mixed with dry or wet air as appropriate to adjust RH. Loadings were applied at each of the three RHs (LRH, MRH, and HRH). The flow was split into three streams toward the filters (Φ, 47 cm; 3M 1870) to deliver 4 liters/min, corresponding to a face velocity of 5.3 cm/s, a standard face velocity for air filter system testing (28). After loading with aerosol for 30 min at the selected RH, the filter was removed and cut into equal quadrants to be prepared for UV exposure. Scanning electron microscopic (SEM; JEOL JSM-6330F; JEOL Inc.) images of filters contaminated with viruses generated in different media were taken and compared to investigate the protective effect of solid components.

UV exposure. During UV exposure, the UV-C lamp (UVG-11; 254 nm, 230 V, 4 W; UV Products, Cambridge, United Kingdom) was adjusted to a height of 10 cm. UV intensity of 1.0 mW/cm^2 was measured using a radiometer (PS-300; Apogee, Logan, UT). The quadrants were placed on a petri dish in a chamber and exposed to UV for different exposure times (0 to 2 h) at the selected RH. One quadrant used as a control was not exposed to UV; the other three were exposed to UV for different times. All were evaluated after the maximum exposure time for a fair comparison.

Dry/wet air was fed into the chamber to adjust the relative humidity in the system. After the maximum exposure time, each quadrant was placed in a 50-ml conical tube containing sterilized DI water and agitated with a wrist action shaker (Model 75; Burrell Scientific, PA) inclined 20° for 15

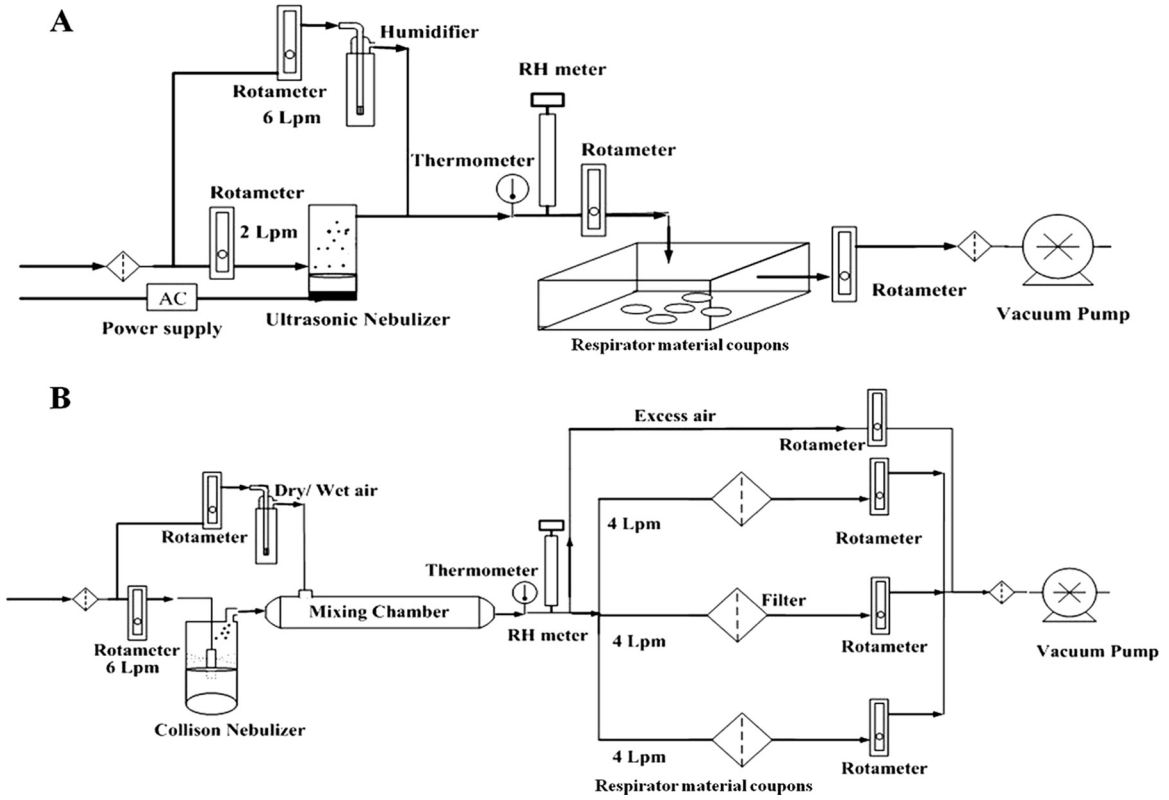

FIG 1 Schematic diagrams of the droplet loading system (A) and aerosol loading system (B).

min to extract MS2. The extracted MS2 was assayed with the single-layer method. IE was determined by comparing the count from the irradiated coupon to that from the paired control:

$$\mathrm{IE} = \frac{PFU_{\mathrm{ctl}}}{PFU_{\mathrm{exp}}} \quad (1)$$

Triplicate tests for each condition and duplicate assays were conducted. Two-way analysis of variance (ANOVA) and three-factor ANOVA were used for statistical analysis (Design-Expert 8.0). The coefficient of variation of amounts loaded on the quadrants was less than 20%.

RESULTS AND DISCUSSION

Effect of transmission mode with different media. Log IE is plotted in Fig. 2 as a function of UV irradiation time for both droplet and aerosol modes with three different nebulization media. HRH was applied for both loading and UV irradiation. For droplet transmission mode, the log IEs were 4.32, 2.32, and 1.98 after 60-min irradiation in DI water, AS, and BE, respectively, whereas for aerosol transmission mode, the log IEs were 5.01, 2.68, and 2.32 in DI water, AS, and BE, respectively. Vo et al. (30) showed that approximately 3 log IE was achieved in 271 B medium applying 4.32 J/cm^2 under MRH during UV exposure, whereas at the same power density and RH condition in this study, 5.2, 3.0, and 2.7 log IEs were measured in DI water, AS, and BE, respectively, for aerosol transmission mode, and 4.8, 2.7, and 2.5 log IEs in DI water, AS, and BE, respectively, for droplet transmission mode.

The IEs in Fig. 2 depend on the following three parameters.

(i) UV irradiation time. At a wavelength of 254 nm, a UV-C photon striking a biological cell is selectively absorbed by one of adjacent pairs of nucleotide bases, thymine in DNA or uracil in RNA, causing them to form covalent bonds with each other and interrupting hydrogen bonds with adenine bases in the cDNA/RNA strain (13, 18). Pyrimidine dimers of thymine/uracil bases distort the shape of DNA/RNA, altering the double-helical structure and preventing the cell's accurately transcribing or replicating its genetic material, which ultimately leads to the death of the cell (13, 18, 19). Extending the irradiation time increased the IE

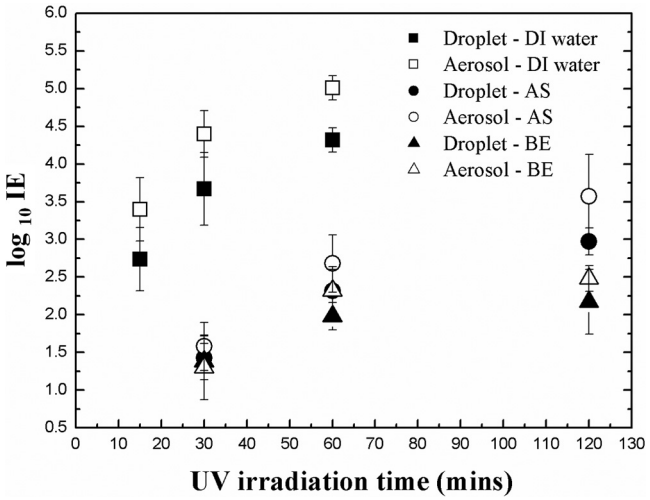

FIG 2 Log IE after virus loading and UV exposure at HRH for droplet and aerosol transmission modes as a function of UV irradiation time in different nebulizer media.

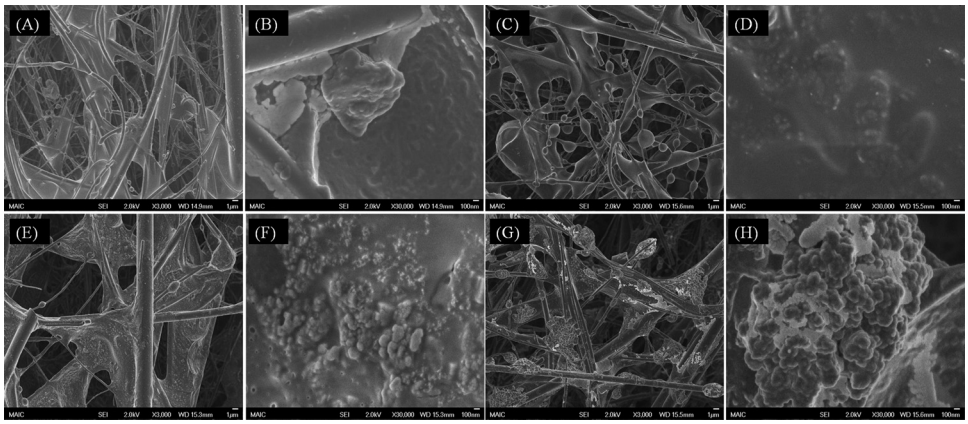

FIG 3 SEM images of filters loaded with viruses aerosolized from DI water (A and B), 0.3% beef extract (C and D), artificial saliva (E and F), and mucin-free artificial saliva (G and H). (A, C, E, and G) Magnification, ×3,000. (B, D, F, and H) Magnification, ×30,000.

because the UV dose (UV-C photon) increased. When the application time was changed from 30 to 60 min, the dose of UV irradiation doubled from 1.8 to 3.6 J/cm^2, increasing the amount of damage to nucleic acids.

(ii) Transmission mode. IE for aerosols was higher than for droplets. Water in the droplets absorbs UV (13, 18), and shielding of viruses near the center of the aggregate likely also contributes to this trend. The size of droplets generated from the ultrasonic nebulizer was around 9 to 10 μm (33), whereas aerosols from the Collison nebulizer measured 1 to 2 μm (16). The evaporation time for a 1-μm droplet at HRH is 0.0077 s at 20°C. As the residence time of aerosol in the mixing chamber was 0.21 s, these particles reached equilibrium during transit. However, the evaporation time of 9- to 10-μm droplets at HRH and 20°C, 0.63 to 0.7 s, is much longer than the residence time. Therefore, the larger droplets retain much of their water at contact.

The equation for evaporation time is the following (11):

$$t_{\text{evaporation time}} = \frac{R\rho_p d_d^2}{8D_v M\left(\frac{p_d}{T_d} - \frac{p_\infty}{T_\infty}\right)} \quad (2)$$

where R is the ideal gas law constant, ρ_p is the density of the particle, d_d is the droplet size, D_v is the diffusion coefficient of water vapor molecule, M is the molecular weight of water, T_∞ and p_∞ are the temperature and pressure away from the droplet surface (i.e., the environmental conditions), respectively, and T_d and p_d are those at the droplet surface. Room temperature (20°C) was applied for T_∞, and the equation below was used to determine T_d.

$$T_d = T_\infty + \frac{(6.65 + 0.345T_\infty + 0.0031T_\infty^2)(S_R - 1)}{1 + (0.082 + 0.00782T_\infty)S_R} \quad (3)$$

where S_R is the saturation ratio. The partial pressure in kPa at a given temperature in K was calculated according to

$$p_d = \exp\left(16.7 - \frac{4{,}060}{T_d - 37}\right) \quad (4)$$

(iii) Spraying medium. IEs in AS and in BE were much lower than in DI water for both aerosol and droplet transmissions. The likely reason for this difference is a protective effect caused by solids in both AS and BE. Based on the composition of the media, the volume fractions of solids in DI water, BE, and AS were 1×10^{-4}, 3.1×10^{-3}, and 6.0×10^{-3}, respectively, after complete evaporation. DI water has a much lower solid content. This mode of protection is supported by SEM images, shown in Fig. 3, of filters contaminated with MS2 viruses aerosolized in different media. Images of MS2 generated in DI water and loaded on the filter (Fig. 3B) show aggregates in the range of 100 nm to 1 μm on the substrate. Riemenschneider et al. (22) and Jung et al. (12) reported MS2 aggregates of around 200 nm for the MS2 suspension and 30 to 200 nm for captured aerosol particles.

MS2 aerosolized in BE instead of DI water was captured as oval-to-spherical features as shown in Fig. 3C. As displayed in Fig. 3D, precipitated BE solids formed a thick shell encapsulating the MS2 virions and/or aggregates. The solids in AS are water-insoluble mucin and various water-soluble salts. To test the hypothesis that the salts and mucin act separately to afford protection (14), MS2 was aerosolized from AS media prepared both with and without mucin. As aerosolized virions and aggregates load onto the filter, it is possible for them to form a wide size range of superaggregates. Figure 3H shows that grape-shaped superaggregates were observed in the absence of mucin. Multivalent cations of the soluble salts (Mg^{2+} and Ca^{2+}) can interact with negatively charged features on the surface of MS2 to promote a high degree of virus aggregation (24). Encasement by a thin layer through the cross-linking network (Fig. 3F) appears to result from gel formation caused by the presence of mucin. The similarity of the underlying structures in Fig. 3F and H suggests that mucin contributes little or nothing to the aggregation process and simply covers the final configuration.

To isolate the UV protection effect of water-insoluble mucin in AS, the IEs of MS2 nebulized in mucin-free AS medium and mucin medium were investigated. For fair comparison, 0.3 and 0.6% of volume fractions were considered. As shown in Fig. 4, for a volume fraction of 0.3%, the log IEs in 0.3% mucin-free AS were 3.66, 4.33, and 4.94 after 30, 60, and 120 min of irradiation, respectively, whereas the log IEs in 0.3% mucin medium were 3.12, 3.94, and 4.37 after 30, 60, and 120 min of irradiation, respectively. The lower log IEs in mucin-free AS compared to those in DI water suggest a protective effect of water-soluble salts, although the difference between 0.3 and 0.6% mucin-free AS was not significant. The log IEs in 0.3% mucin-free AS were higher than those in 0.3% mucin medium (salt-free AS), indicating better protection by water-insoluble mucin than by various water-soluble salts. Relatively

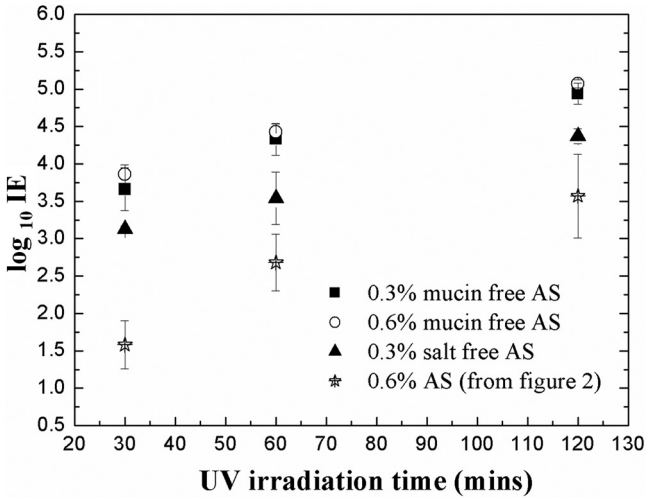

FIG 4 Log IE after virus loading and UV exposure at HRH for aerosol transmission mode as a function of UV irradiation time in 0.3 and 0.6% mucin-free artificial saliva and 0.3% salt-free artificial saliva.

TABLE 1 Statistics in general factor ANOVA[a]

Factor	*P* value
Three-factor ANOVA for three media	
Spray medium	<0.0001*
RH during UV inactivation	0.0197*
RH during aerosol loading	<0.0001*
Spray × RH during aerosol loading	<0.0001*
Two-way ANOVA for DI water	
RH during aerosol loading	<0.0001*
RH during UV inactivation	<0.0001*
RH during UV inactivation × RH during aerosol loading	0.0118*
Two-way ANOVA for beef extract	
RH during aerosol loading	0.2202
RH during UV inactivation	0.4188
RH during UV inactivation × RH during aerosol loading	0.6278
Two-way ANOVA for artificial saliva	
RH during aerosol loading	0.4569
RH during UV inactivation	0.0204*
RH during UV inactivation × RH during aerosol loading	0.9983

[a] An asterisk indicates a significant parameter.

higher IEs in both mucin-free AS and salt-free AS than those in AS suggest that both encasement by water-insoluble mucin and aggregation by water-soluble salts contribute protection. In addition, that the encasement in BE provided better protection than in AS, even though the volume fraction of solids in BE is only half of that in AS, appears to indicate that the organic solids in BE are stronger absorbers at 254 nm and thus provide more effective protection from UV radiation.

Effect of RH during both loading and inactivation. Log IEs measured after aerosol loading for 30 min, followed by UV exposure for 60 min at different RHs, are displayed in Fig. 5; the corresponding general-factor ANOVA results appear in Table 1. Because the strong effect of the spray medium (>80% contribution; data not shown) made it difficult to distinguish the RH effect, two-way ANOVA was also conducted for each spray medium. For the data shown in Fig. 5, upon completion of the experiment, the highest inactivation efficiency, around log 5.8, was seen in filters subjected to UV after applying the MS2 in DI water at LRH. However, it should be noted that the actual IE at this condition might be somewhat higher, because values measured under LRH during UV inactivation after aerosol loading in both LRH and MRH conditions were at the detection limit of our experimental system.

For MS2 delivered in DI water, both RH during UV inactivation ($P < 0.0001$) and RH during aerosol loading ($P < 0.0001$) are significant, as is the interaction for both RHs ($P = 0.0118$). This may be attributed to a combination of intrinsic susceptibility of MS2 and UV exposure susceptibility of MS2, augmented by stress imposed on MS2 by aerosolization under different loading RHs. The second susceptibility was the more important parameter, because the contribution of RH during inactivation (75%; data not shown) was five times that of RH during aerosol loading (15%; data not shown). In general, IEs at LRH were higher than those at both MRH and HRH, suggesting a protective contribution by a water layer. This is broadly consistent with a report that inactivation efficiency of UV against microbes dramatically dropped off above 70% RH (3).

Unlike in DI water, IEs in BE were not significantly influenced by RH during virus loading, during UV irradiation for 60 min, or

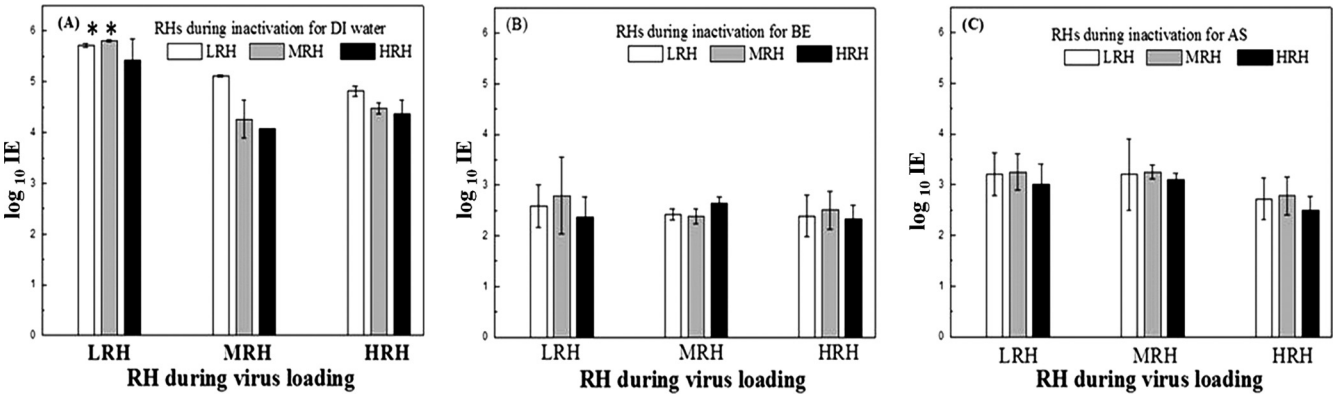

FIG 5 Log inactivation efficiency as a function of relative humidity during both loading and UV inactivation in DI water (A), 0.3% beef extract (B), and artificial saliva (C).

TABLE 2 Virus susceptibility factor K under different conditions for aerosol transmission

RH loading and UV exposure	K (m^2/J) in:		
	DI water	AS	BE
LRH			
LRH	0.764	0.056	0.046
MRH	0.267	0.043	0.040
HRH	0.273	0.045	0.039
MRH			
LRH	0.222	0.061	0.051
MRH	0.189	0.058	0.044
HRH	0.209	0.051	0.041
HRH			
LRH	0.231	0.055	0.042
MRH	0.222	0.056	0.044
HRH	0.207	0.044	0.038

TABLE 3 Comparison of virus susceptibility factor K (m^2/J) from other studies and technologies

Test microbe	DNA type[a]	K (m^2/J) at:		Reference or source
		<68% RH	>75% RH	
Adenovirus	dsDNA	0.039	0.068	31
Vaccinia virus	dsDNA	6.01	1.42	17
Phage T7	dsDNA	0.33	0.22	27
Phage phi 6	dsRNA	0.43	0.31	27
Phage phi X174	ssDNA	0.71	0.53	27
Coronavirus	ssRNA	0.38		31
MS2[b]	ssRNA	0.19–0.76	0.21–0.27	This study

[a] ds, double stranded; ss, single stranded.
[b] DI water was the spray medium.

by their interaction. IE was in the range of 2.4 to 2.8 logs under all nine sets of RH conditions. The contributions of both RH regimens are less than 6%, although the contribution of RH during inactivation is 1.9 times that of RH during virus loading, suggesting some effect of water on protection by the solid content. To investigate the protective effect of solid contents in BE directly, we compared the intensities of 1.0-mW/cm^2 UV beams after penetration of BE solutions of different concentrations. Values of 0.97, 0.78, 0.62, and 0.41 mW/cm^2 were found after penetration of solutions containing 0, 0.1, 0.3, and 0.5% BE, respectively, verifying the conclusion above that UV absorbers in BE contribute significantly to its observed protective effect.

In AS, IEs fell to the range of 2.7 to 3.2 logs under all conditions, showing that dissolved solids in these experiments eliminated sensitivity of the MS2 particles to RH during loading. However, RH during inactivation was a statistically significant factor ($P = 0.0204$). In AS, to distinguish the significance of the RH levels, a Tukey comparison was conducted and a difference was identified at HRH. Compared to BE, AS was less protective even though the solid fraction of AS is larger, and the contribution of RH at both stages was greater in AS (38%; not shown) than in BE (6%; not shown). These findings are consistent with conclusions described above from SEM images and UV absorption results that the two solid media act by different routes. Solids in BE appear to encase the virions in a shell that provides environmental protection and some UV screening. In contrast, multivalent cations in AS appear to gather virions and promote formation of superclusters that are coated with a layer of mucin as a gel, which affords less protection and is more sensitive to water than the BE shell.

Virus susceptibility. When microbes are exposed to a biocidal factor, first-order decay of viability is commonly observed (1), and the IE of UV irradiation as a function of time can be defined as

$$\mathrm{IE} = \frac{N_o}{N_s} = (A \times e^{-KCt})^{-1} \quad (5)$$

where A is the fraction of the total initial population subject to fast decay, N_s is the concentration of airborne virus surviving after UV exposure, N_o is the concentration of airborne virus before UV exposures, C is the UV intensity factor (W/m^2), t is time (s), and K is the virus susceptibility factor (m^2/J).

Although this equation gives a straight line in a semilogarithmic representation, two characteristics at the beginning and end (e.g., shoulder [IE, <90%] and tailing) were not incorporated (3, 13). The shoulder represents the threshold dose; if the dose is insufficient, the virus shows negligible response or even recovers from the damage. Meanwhile, the slow decay curve at tailing might be from a resistant minority of viruses and/or reaching the detection limit (13).

Table 2 lists the first-order decay, K_s, derived from the experimental results. A higher K was observed for both loading and exposure in LRH. In addition, and as expected, K at LRH in DI water was higher (by more than 10×) than in AS or BE. Reported UV susceptibilities of some other viruses are listed in Table 3. K for viruses is in the range of 0.01 to 10. The value of MS2 in DI water is similar to that for coronavirus, which is of the same genomic type. Low K values for double-stranded and DNA-type viruses were expected both because their undamaged strands are able to repair UV-damaged segments and because RNA is a stronger UV absorber than DNA (13, 18). However, for the double-stranded DNA (dsDNA) type, values of K were found to vary widely, depending on the individual characteristics of viruses rather than following a simple classification by genome type.

ACKNOWLEDGMENTS

This research was supported by the Air Force Research Laboratory through grant FA 8650-06-C-5913. Myung-Heui Woo and Adam Grippin acknowledge an Alumni Scholarship and Undergraduate Research Scholarship supported by the HHMI Science for Life Program, respectively, at the University of Florida.

We are grateful to the Major Analytical Instrumentation Center at the University of Florida for providing the SEM.

REFERENCES

1. **Brickner P, et al.** 2003. The application of ultraviolet germicidal irradiation to control transmission of airborne disease: bioterrorism countermeasure. Public Health Rep. **118**:99–114.
2. **Brion GM, Silverstein J.** 1999. Iodine disinfection of a model bacteriophage, MS2, demonstrating apparent rebound. Water Res. **33**:169–179.
3. **Burgener J.** 2006. Position paper on the use of ultraviolet lights in biological safety cabinets. Applied biosafety. J. Am. Biol. Safety Assoc. **11**:228–230.
4. **CDRF.** 2006. Reusablility of facemasks during an influenza pandemic: facing the flu. National Academies Press, Washington, DC. http://www.nap.edu/catalog.php?record_id=11637.
5. **Chuaybamroong P, Thunyasirinon C, Supothina S, Sribenjalux P, Wu CY.** 2011. Performance of photocatalytic lams on reduction of culturable airborne microorganism concentration. Chemosphere **83**:730–735.
6. **Cote RJ.** 1999. Media composition, microbial, laboratory scale, p 104–

122. *In* Flickinger D (ed), Encyclopedia of bioprocess technology: fermentation, biocatalysis, and bioseparation. John Wiley & Sons, Inc., New York, NY.
7. **Drazen JM.** 2002. Smallpox and bioterrorism. N. Engl. J. Med. **346**:1262–1263.
8. **EPA.** 1984. USEPA manual methods for virology. U.S. Environmental Protection Agency, Research and Development, 600/4-84-013, Cincinnati, OH. http://www.epa.gov/microbes/chap4.pdf.
9. **Fisher E, Rengasamy S, Viscusi D, Vo E, Shaffer R.** 2009. Development of a test system to apply virus containing particles to filtering facepiece respirators for the evaluation of decontamination procedure. Appl. Environ. Microbiol. **75**:1500–1507.
10. **Heimbuch B, et al.** 2010. A pandemic influenza preparedness study: use of energetic methods to decontaminate filtering facepiece respirators contaminated with H1N1 aerosols and droplets. Am. J. Infect. Control **39**:e1–e9. doi:10.1016/j.ajic.2010.07.004.
11. **Hinds WC.** 1999. Aerosol technology. John Wiley and Sons, Inc., New York, NY.
12. **Jung JH, Lee J, Kim S.** 2009. Generation of nonagglomerated airborne bacteriophage particles using an electrospray technique. Anal. Chem. **81**:2985–2990.
13. **Kowalski W.** 2009. Ultraviolet germicidal irradiation handbook. Springer, New York, NY.
14. **Lee JH, et al.** 2009. Assessment of iodine-treated filter media for removal and inactivation of MS2 bacteriophage aerosols. J. Appl. Microbiol. **107**:1912–1923.
15. **Lee IS, et al.** 2011. Aerosol particle size distribution and genetic characteristic of aerosolized influenza A H1N1 virus vaccine particles. Aerosol Air Qual. Res. **11**:230–237.
16. **May KR.** 1973. The collision nebulizer: description, performance and application. J. Aerosol Sci. **4**:235–238.
17. **McDevitt JJ, et al.** 2007. Characterization of UVC light sensitivity of vaccinia virus. Appl. Environ. Microbiol. **73**:5760–5766.
18. **Miller RL, Plagemann PGW.** 1974. Effect of ultraviolet light on mengovirus: formation of uracil dimer linkage of protein to viral RNA. J. Virol. **13**:729–739.
19. **Perier C, Bové J, Vila M.** 2011. Mitochondria and programmed cell death in Parkinson's disease: apoptosis and beyond. Antioxid. Redox Signal. **16**:883–895. doi:10.1089/ars.2011.4074.
20. **Prescott LM, Harley JP, Klein DA.** 2006. Microbiology. McGraw-Hill Companies, Inc., New York, NY.
21. **Rengasamy S, Fisher E, Shaffer R.** 2010. Evaluation of the survivability of MS2 viral aerosols deposited on filtering face piece respirator samples incorporating antimicrobial technologies. Am. J. Infect. Control **38**:9–17.
22. **Riemenschneider L, et al.** 2010. Characterization of reaerosolization from impingers in an effort to improve airborne virus sampling. J. Appl. Microbiol. **108**:315–324.
23. **Ryan K, McCabe K, Clements N, Hernandez M, Miller S.** 2010. Inactivation of airborne microorganisms using novel ultraviolet radiation sources in reflective flow-through control devices. Aerosol Sci. Technol. **44**:541–550.
24. **Schaffer FL, Soergel ME, Straube DC.** 1976. Survival of airborne influenza virus: effects of propagating host, relative humidity, and composition of spray fluids. Arch. Virol. **51**:263–273.
25. **Sjogren J, Sierka R.** 1994. Inactivation of phage MS2 by iron-aided titanium dioxide photocatalysis. Appl. Environ. Microbiol. **60**:344–347.
26. **Tabak LA.** 1995. In defense of the oral cavity: structure, biosynthesis, and function of salivary mucin. Annu. Rev. Physiol. **57**:547–564.
27. **Tseng C, Li CS.** 2005. Inactivation of virus containing aerosols by ultraviolet germicidal irradiation. Aerosol Sci. Technol. **39**:361–366.
28. **United States Army.** 1998. Filter medium, fire-resistant, high efficiency, military specification MIL-F-51079D. U.S. Army Armaments Munitions and Chemical Commands, Aberdeen Proving Ground, MD. www.wbdg.org/ccb/FEDMIL/f51079d.pdf.
29. **Viscusi DJ, Bergman MS, Eimer BC, Shaffer RE.** 2009. Evaluation of five decontamination methods for filtering facepiece respirators. Ann. Occup. Hyg. **53**:815–827.
30. **Vo E, Rengasamy S, Shaffer RE.** 2009. Development of a test system to evaluate procedures for decontamination of respirators containing viral droplets. Appl. Environ. Microbiol. **75**:7303–7309.
31. **Walker CM, Ko G.** 2007. Effect of ultraviolet germicidal irradiation on viral aerosol. Environ. Sci. Technol. **41**:5460–5465.
32. **Woo MH, Hsu YM, Wu CY, Heimbuch B, Wander J.** 2010. Method for contamination of filtering facepiece respirators by deposition of MS2 viral aerosol. J. Aerosol Sci. **41**:944–952.
33. **Woo MH, et al.** 2011. Evaluation of the performance of dialdehyde cellulose filters against airborne and waterborne bacteria and viruses. Ind. Eng. Chem. Res. **50**:11636–11643.
34. **Zhang Q, et al.** 2010. Microwave assisted nanofibrous air filtration for disinfection of bioaerosols. J. Aerosol Sci. **41**:880–888.